

Instability of MRE film – substrate block under magneto-mechanical loadings

E. Psarra¹, K. Danas¹, L. Bodelot¹

¹ Laboratoire de Mécanique des Solides (LMS), Ecole Polytechnique, {psarra,danas,bodelot}@lms.polytechnique.fr

Résumé — The present study pertains to the bifurcation modes of a MRE film bonded on a non-linear elastic and highly compliant substrate. The motivation derives from the increasing development of the magneto-sensitive elastomers and the magnetically triggered instabilities, possibly applicable in actively controlled haptic systems. The present study introduces a fully featured magneto-mechanical experiment that yields different film surface patterns, being activated by low magnetic fields and proper pre-straining of the bilayer system.

Mots clés — MRE, instability, magneto-mechanical coupling

1 Introduction

Magneto-rheological elastomers (MRE) are ferromagnetic particle impregnated elastomers, whose mechanical properties are altered by the application of external magnetic fields. They belong to the class of the ‘active materials’, being able to respond in a pre-determined manner to given environmental stimulations, exhibiting inherent macroscopic changes, while reverting back to their original state, as soon as the stimulus is removed¹. The reversibility and repeatability of their response, combined with a strong multi-physics coupling, render them applicable in sensors and actuators. However, one of the most restrictive parameters in finding new applications – or widen the already known – is the usually high magnetic fields required to achieve an efficient active control.

A primary structure, which is possible to cope with analytically and fabrication wise, is the stiff film-soft substrate block. Such systems are known to undergo mechanical instabilities, leading to the formation of surface patterns. In fact, literature provides several examples of such bilayers that buckle under purely compressive mechanical loads, while the critical loads and modes depend on the applied loads, the geometrical features of the structure, the material properties of the constitutive phases and others².

The present study aims at exploiting the magneto-elastic coupling of such a system, since wrinkling can be a result of coupled magneto-mechanical loadings³. Hence, the basic idea is to bring the structure near (but not at) a mechanical critically stable state and then destabilize it with a small magnetic field (Figure 1a).

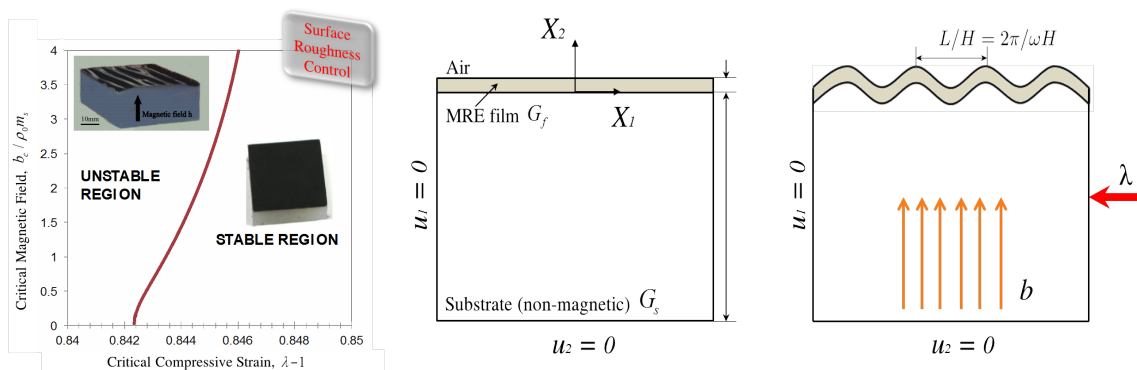


FIGURE 1 – (a) Qualitative stability phase diagram of the MRE film-substrate block ; (b) Pre and post-bifurcation regime of the block after the application of magneto-mechanical loadings

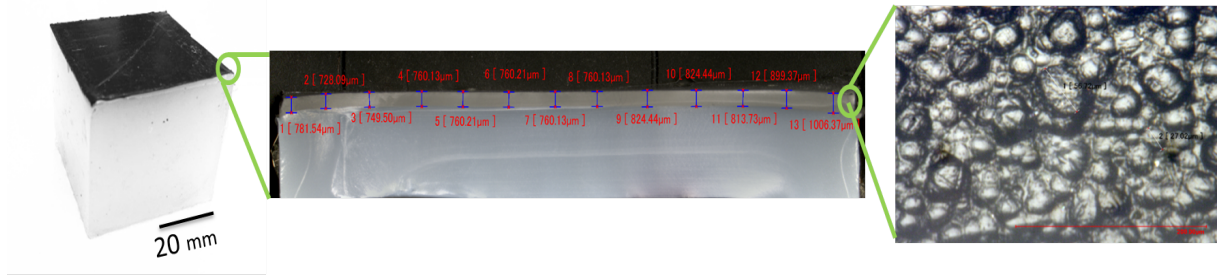


FIGURE 2 – (a) The MRE film-substrate block specimen ; (b) Microscopic topography of the MRE film-substrate block ; (c) MRE film microstructural morphology by Keyence Microscopy, 30% particle volume fraction

The magnetic field is always applied in the direction of the film thickness, while the stretch is applied along the interface direction (Figure 1b). Subsequently, a stable post-bifurcation mode of finite and controllable wavelength is obtained. In order to do so, the boundary value problem and the post-bifurcation evolution have to be numerically solved, so as to determine the constitutive material properties and the critical loads needed to trigger and control the instability. Novel manufacturing and experimental procedures have to be put in place, driven by the simulation (FE) analysis and the analytical study of the film-substrate problem. The present study introduces a fully featured magneto-mechanical experiment that yields the MRE film finite wrinkling, being activated by low magnetic fields and proper pre-straining of the film-substrate system.

2 Fabrication

The substrate and the film are fabricated using standard silicones (e.g., ECOFLEX Shore). The reinforcing spherical particles are in form of carbonyl iron powder and have an average diameter of $5\mu\text{m}$. The filler volume fractions is 25%. The materials are manufactured in the absence of magnetic field, hence leading to isotropic MREs. The manufacturing process is a typical cross-linked polymer obtained by 3 min mixing and 7 min degassing. To cast the material into the $40 \times 40 \times 40$ (mm^3) aluminum mold, we first pour the film and immediately after the substrate on the top of the film. Electrical resistances are attached on the cubic mold, so as the polymerization of the film and substrate take place simultaneously. The bilayer is subjected to a 60 min thermal processing at 70°C . By means of optical microscopy, we verify a quasi-constant film thickness at 0.8mm and an almost perfect adhesion between the film and the substrate (Figure 2).

3 Experiments

Purely mechanical, purely magnetic and combined magneto-mechanical tests are carried-out to experimentally reveal the wrinkling effect. The magneto-mechanical experiment takes place into a 0.8 T maximum amplitude electro-magnet, while the pre-stretch is applied by a 3D printed compression device, able to be incorporated into the magnet. The specimen is first compressed and then installed in between the poles of the magnet, where the field subsequently increases from 0 to 0.7 T in a ramp way.

Figure 3 shows the critical modes of the block in the parameter space of the magnetic field \mathbf{b} and the mechanical pre-compression λ . As seen, for a given pre-stretch ratio at 0.8, we obtain magnetically activated wrinkling that remains stable versus the magnetic field. Remarkable is also the response of the bilayer for two extreme cases ; low and high stretches, e.g., $\lambda = 0.93$ and 0.73 respectively. For very low compressive values, i.e., $\lambda = 0.93$, the post bifurcation evolution is mainly defined by 3D effects, i.e., wrinkles running in different in-plane directions. This explains the dark thick layer in the images obtained by the camera in this case, since we do not have access to the 3D top view due to the presence of the magnetic poles. For very high pre-compressions, i.e., $\lambda = 0.73$, the post bifurcation configuration gives an initial mechanical crease, while wrinkles are ‘activated’ at a later time by the magnetic field.

The experimental bifurcation points are defined by means of image processing, after extracting the profile of the film (figure 4a) and calculating the out-of-plane displacements. The average amplitude of

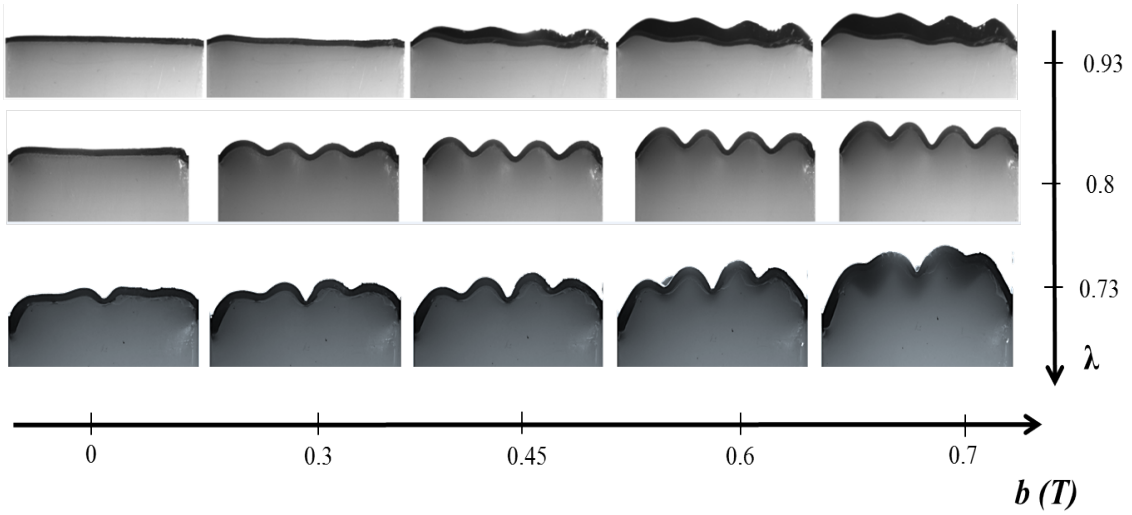


FIGURE 3 – Instability modes of the Shore-0050/ $c=25\%$ CIP MRE film adhered on the Shore-0010 substrate for $40 \times 40 \times 40$ (mm^3) block, of 0.8 mm film thickness, as a function of the magnetic field and the pre-compression.

wrinkling is defined as the average distance of the film peaks from the film vales of the two central wrinkles. This deflection can be traced versus the magnetic field for given pre-stretches, as seen in figure 4b. From this graph, bifurcation points can be identified by setting different thresholds of wrinkling amplitude. Note that the greater the pre-stretch, the sooner the instability emerges, i.e., the lower the magnetic field needed to trigger bifurcation.

4 Theory & Numerics

The continuum formulation proposed is a Langrangian variational approach. It pertains to the minimization of a potential energy function (eq.1), which yields all the appropriate governing equations and boundary/interface conditions⁴. At the heart of the analytical theory lies a phenomenological isotropic free energy density that depends on both elastic (i.e., deformation gradient tensor \mathbf{F}) and magnetic (i.e., magnetic field \mathbf{B}) properties of the materials. Eq. 2 and 3 represent the energy functions for the subatrate/air and the film respectively,

$$P(\mathbf{u}, \mathbf{A}) = \int_V [W(\mathbf{F}, \mathbf{B}) - \rho_0 \mathbf{f} \cdot \mathbf{u}] dV + \int_{R^3 \setminus V} \frac{1}{2\mu_0 J} (\mathbf{FB}) \cdot (\mathbf{FB}) dV - \int_{\partial V} \mathbf{T} \cdot \mathbf{u} dA + \int_{\partial V^\infty} (\mathbf{H} \times \mathbf{A}) \cdot \mathbf{N} dA \quad (1)$$

$$W^{s,a}(\mathbf{F}, \mathbf{B}) = \frac{G_{s,a}}{2} (I_1 - 3 - 2 \ln J) + \frac{G'_{s,a}}{2} (J - 1)^2 + \frac{1}{2\mu_0 J} (\mathbf{FB}) \cdot (\mathbf{FB}) \quad (2)$$

$$W^f(\mathbf{F}, \mathbf{B}) = \frac{G_f}{2} (I_1 - 3 - 2 \ln J) + \frac{G'_f}{2} (J - 1)^2 + \frac{1}{2\mu_0 J} (\mathbf{FB}) \cdot (\mathbf{FB}) + \frac{\mu_0 m_s^2}{3\chi} - \left[\ln \left(\frac{3\chi \sqrt{(\mathbf{FB}) \cdot (\mathbf{FB})}}{\mu_0 m_s J} \right) - \ln \left(\sinh \left(\frac{3\chi \sqrt{(\mathbf{FB}) \cdot (\mathbf{FB})}}{\mu_0 m_s J} \right) \right) \right] \quad (3)$$

where, \mathbf{f} the body force vector, \mathbf{u} the displacement vector, \mathbf{A} the potential vector of the magnetic field, ρ_0 the material density at the initial configuration, G the shear modulus, G' the Lamé modulus, μ_0 the permeability of the air, m_s the saturation magnetization and χ the susceptibility.

To numerically account for the magnetic energy of the air in the potential energy formulation, we have to mesh the surrounding space. The finite element analysis (FEA) considers an isotropically particle filled film laying upon an elastic substrate, for given substrate-to-film thickness ratios, H_s/H_f (figure 5). The FEA simulations are carried out by developing a user-element in the open-source code FEAP.

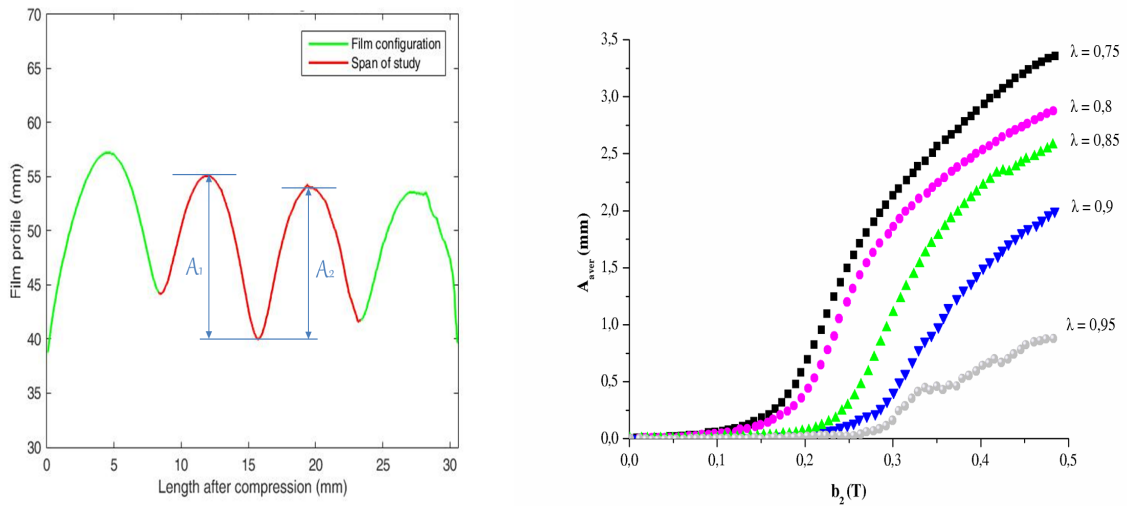


FIGURE 4 – (a) Film profile at a given time. The average amplitude is taken by $A = (A_1 + A_2)/2$; (b) Experimental wrinkling amplitude curves for different pre-stretches.

The geometry of the film–substrate block and the applied loads are the ones used in the experiments. Figure 6a shows the numerical and experimental average amplitude of wrinkling as a function of the magnetic field, for three pre-stretches at 0.85, 0.88 and 0.9. The numerical curves are in a very good agreement with the experimental pre- and post-bifurcation amplitude ones. Moreover, in order to have a global view of the MRE film–substrate response, we present the numerical and experimental instability curves for a threshold at 0.6 mm wrinkling amplitude (figure 6b).

The instability curves show the critical magnetic field needed to initiate the instability as a function of the pre-compression. It is clearly observed the decrease of the onset of bifurcation with increase of the compressive stretch. That is one of the major results and one of the primary goals of the present study. From this figure, we observe that for moderate and low pre-stretches, our FEA is able to capture the experimental bifurcation points, while for high pre-compressions, the numerical results continue to decrease whereas the experimental ones exhibit an asymptotic behavior, with no more reduction of the critical magnetic field. One possible reason for this difference could be the friction present between the lateral faces of the specimen and the walls of the compression device.

5 Conclusions

The present investigation aims at the active control of a surface roughness by exploiting the unstable regime of a critically stable MRE stiff film–soft foundation. The study involves the development of novel fabrication techniques and experimental testing procedures, combined efficiently with advanced theoretical and numerical models and tools. These altogether allow for the analysis of the coupled

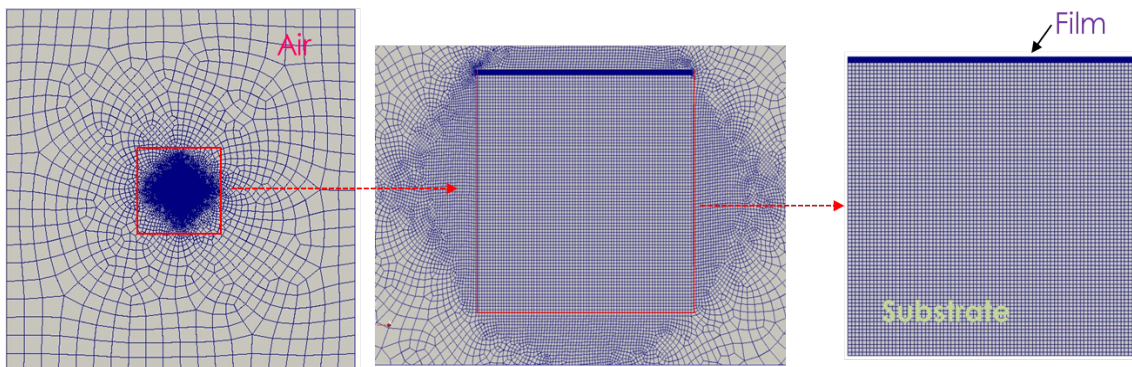


FIGURE 5 – Mesh for the finite element method including the air, the film and the substrate.

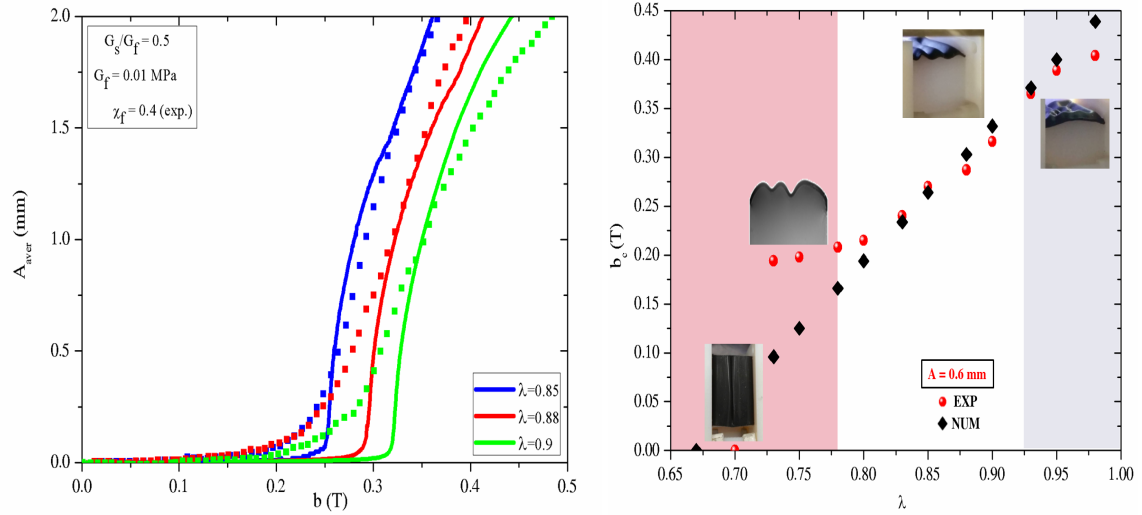


FIGURE 6 – (a) Experimental and numerical wrinkling amplitude curves for different pre-stretches ; (b) Experimental and numerical instability curves with the relevant critical modes, for a threshold at 0.6mm wrinkling amplitude.

magneto–mechanical response of a MRE film/substrate block, which is able to produce well designed and controllable wrinkles, whereby we guide the design of a combined magneto–mechanical wrinkling surface pattern.

To conclude, we have obtained a clear trend of a decreasing critical magnetic field with increase of the mechanical pre-compression. Stable wrinkles were observed in the post-bifurcation regime. Moreover, the numerical analysis has been shown to be in very good agreement with the experimental results in a large range of loads. In turn, the modeling of friction in the lateral faces could possibly improve the comparisons between numerical estimates and experiments at large pre-compressions, where the concomitant presence of mechanical creases and magnetically-induced wrinkles leads to a saturation of the critical magnetic field, with respect to further increase of pre-compression.

6 References

Références

- [1] Takagil, T., 1990. Journal of Intelligent Material Systems and Structures, Volume 1, pp. 149-156.
- [2] Audoly B., Boudaoud, A. : Buckling of a stiff film bound to a compliant substrate. Part I. Formulation, linear stability of cylindrical patterns, secondary. J. Mech. Phys. Solids 56 :2401–2421, 2008.
- [3] Danas K., Triantafyllidis, N. : Instability of a magnetoelastic layer resting on a non-magnetic substrate. J. Mech. Phys. Solids 69 :67–83, 2014.
- [4] Kankanala S., Triantafyllidis, N. : Magnetoelastic buckling of a rectangular block in plane strain. J. Mech. Phys. Solids 56 :1147–1169, 2008.